

Power Inter Cell Transformer Modelling for ASV Application

Guillaume Pellecuer, Thierry Martiré, Loïc Daridon

▶ **To cite this version:**

Guillaume Pellecuer, Thierry Martiré, Loïc Daridon. Power Inter Cell Transformer Modelling for ASV Application. 48th Annual Conference of the Industrial Electronics Society- IECON 2022 Conference, Oct 2022, Bruxelles, France. 10.1109/IECON49645.2022.9968513 . hal-03822881

HAL Id: hal-03822881
https://hal.science/hal-03822881

Submitted on 20 Oct 2022

HAL is a multi-disciplinary open access archive for the deposit and dissemination of scientific research documents, whether they are published or not. The documents may come from teaching and research institutions in France or abroad, or from public or private research centers.

L'archive ouverte pluridisciplinaire **HAL**, est destinée au dépôt et à la diffusion de documents scientifiques de niveau recherche, publiés ou non, émanant des établissements d'enseignement et de recherche français ou étrangers, des laboratoires publics ou privés.

Power Inter Cell Transformer Modelling for ASV Application

Guillaume PELLECUER
LMGC - IES
Université de Montpellier, CNRS
Montpellier, FRANCE
guillaume.pellecuer@umontpellier.fr

Thierry MARTIRÉ
IES
Université de Montpellier, CNRS
Montpellier, FRANCE
thierry.martire@umontpellier.fr

Loïc DARIDON
LMGC
Université de Montpellier, CNRS
Montpellier, FRANCE
loic.daridon@umontpellier.fr

***Abstract*—This paper deals with the design of a power intercell transformer (ICT) for a marine drone application. This on-board converter, with a power of the order of kW, is intended to adapt the energy coming from the solar panels to recharge the on-board battery of the vehicle. The constrained application requires special attention to the design of this intercell power transformer. The dimensioning approach by 3D finite element modeling is then essential to apprehend the complexity of the realization of this type of component and to determine the electromagnetic parameters such as the serial resistances of the windings or the proper and mutual inductances of the ICT. The component, thus dimensioned, has been manufactured and the experimental measurements are compared with those from the modeling.**

***Index Terms*—Marine Autonomous Surface Vehicle, Interleaved converters, Inter Cell Transformer, 3D modeling.**

I. Introduction

The development of marine UAV (Unmanned Aerial Vehicle) and Autonomous Surface Vehicle (ASVs) are widely used to perform a number of different missions. For example, surveillance of human activity (security, offshore exploration, defense of protected areas ...) or environmental monitoring (oceanographic surveys, monitoring of marine wildlife, regulation of fishing areas ...). This new type of boat can accomplish a number of diverse and varied missions while being autonomous. Fig. 1 shows a prototype of an autonomous surface vehicle.

The energy issues related to the use of this type of vehicle are important. Indeed, they must be capable of fulfilling constraining missions during a long time. The management of energy on board is then an essential element in the development of this type of vehicle and more particularly the exploitation of the photovoltaic panels energy. Indeed, this photovoltaic energy is very variable in time and must be connected to the onboard network to charge the batteries or be used by the onboard equipment. The power conversion stage must then allow to maintain a reference output voltage in spite of a variable input source. In addition, size and weight are major considerations in the development of autonomous surface vehicles.

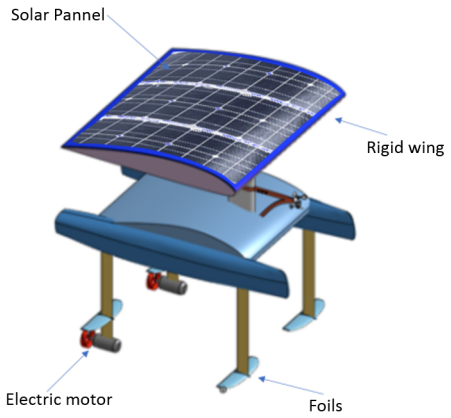


Fig. 1: Autonomous Surface Vehicle

The development of power converters with a high efficiency, a high power density, robust and a high performing in terms of size is perfectly in line with the problem of energy management on board autonomous surface vehicles. The use of a multilevel power converter is particularly suitable for this type of application [1][2]. The on-board network fixed at $48\,\mathrm{V}$ and the variable voltage on input requires the use of a buck boost converter whose structure is visible in Fig. 2.

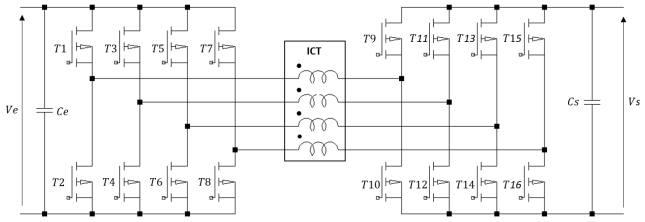


Fig. 2: Buck Boost Interlevead Converter

The Intercell Transformer (ICT) is the key component of this converter. It makes it possible to reduce the losses in the converter and to improve the quality of the energy supplied by a reduction of the current ripples [3][4]. In addition, by the phenomenon of compensation of the magnetic flows, the total volume is found to be reduced compared to a conventional

structure [5]. The dimensioning of this component is then essential to apprehend the realization of this converter. The 3D modeling thus makes it possible to dimension the component and to extract the electromagnetic quantities [6].

This document is dedicated to the 3D modelling approach using the finite element method of the magnetic component. The purpose of such a modelling is to be able to extract the electromagnetic parameters of the ICT such as self and mutual inductance in order to be able to use them in a circuit simulation software where the whole converter can be simply modelled. The first part presents the basic notions of the magnetic component realisation. A second part is devoted to the principles of modelling such a component before continuing with a presentation of the results of this modelling. Finally, before concluding, a comparison between the experimental results and the modelling allows the approach to be validated.

II. Studied 4-phases ICT

A. Presentation of the magnetic component

From high powers, the designer of power structures needs to parallelize the structures. Interleaved structures with separate inductors play this role perfectly. These structures allow to have an efficient filtering while improving the static and dynamic performances, but on the contrary, they present the disadvantage of having important current ripples in each phase. These important ripples in each phase lead to an increase of the RMS current in each phase and thus the losses by Joule effect [7]. This aspect limits the use of this type of converter. A solution then consists in coupling the inductances together using a Inter Cell Transformer (ICT) [8].

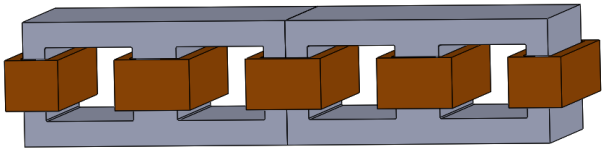


Fig. 3: Intercell Transformer

In the framework of the marine drone project, a separate 4-phases ICT was chosen as part of the Buck-Boost structure of the photovoltaic panel converter. The use of this component allows to improve the performances, but the disadvantage lies in the manufacturing of this magnetic component which is particularly difficult. Indeed, the realization of a customized magnetic component requires very often to cut the ferrite and to assemble each part by gluing. This aspect then limits the performances of the component by a modification of the magnetic properties of the ICT. The coupler presented here, was realized by assembling elementary magnetic structure of type E with 3C90 materials.

The Fig. 3 shows the 4-phases ICT formed from four cores of shape ”E”. The ”E” shaped core combination allows to have five winding ”legs”. The three central ”legs” have the same effective cross section while the outer legs have an area equal to half the cross section of a central leg. The number of turns is identical for three central phases and the double for the last phase. However, this last phase is equally distributed on the two external ”legs”. In this way, the system corresponds to a 4-phase ICT whose magnetic inductances seen by each phase are similar.

The Fig. 4 shows the distribution of the windings within the magnetic circuit. The coils are wound in the same direction and the voltage supplies are shifted by $2\pi/4$ which allows a compensation of the magnetic fluxes. The coils 2, 3, 4 have a number of turns Ns while the two half coils forming the coil 1 are composed of a number of turns Ns each, because the reluctance of the outer leg is double in comparison of a central leg because the section is divided by two. This allows to have equivalent inductances for each phase.

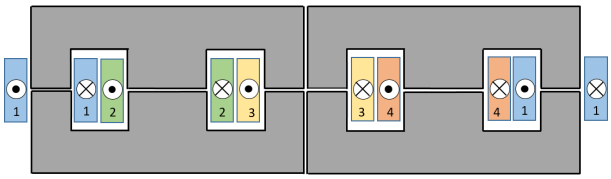


Fig. 4: Ladder magnetic couplers

Designing an inductor involves choosing a compromise between high frequency performances relative to current ripples and DC specifications [9]. Indeed, it is desirable to have a high value inductance to reduce the high frequency current ripple. However, a high inductance crossed by the average current leads to an important energy storage. This energy is proportional to the value of this inductance.

It is then imperative to perfectly master the inductance values. In the case of an ICT, the high frequency role is ensured by the magnetic core part while the continuous behavior is mainly linked to the leakage flux. The control of the self and mutual inductances becomes then obligatory.

In view of the complexity of the geometry studied, the uncertainty of the magnetic quantities of the circuit, and the difficulty of perfectly mastering the protocol of gluing of E-shaped cores, the analytical calculation of the inductance matrix is impossible. The use of numerical modeling using the finite element method seems to be a solution to establish the parameters of the studied ICT (inductances).

B. Matrix reprsentation of 4-phases ICT

The system studied here can be characterized magnetically in matrix form using its inductance matrix. The flux in a ”leg” corresponds to a clean flux generated by the self-inductance and a flux due to the existence of a mutual inductances linked

to the other windings [10]. The Fig. 5 shows the distribution of self-inductance and mutual inductances with respect to the flux in phase 1.

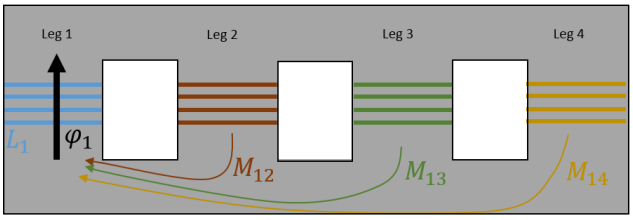


Fig. 5: Self and mutual inductances related to "leg" 1 winding

The flow in phase 1 can then be written :

$$\varphi_1 = L_1.i_1 + M_{12}.i_2 + M_{13}.i_3 + M_{14}.i_4 \tag{1}$$

By doing the same for the three others windings, we can obtain the (4x4) matrix of inductances of this ICT.

$$\begin{pmatrix} L_1 & M_{12} & M_{13} & M_{14} \\ M_{21} & L_2 & M_{23} & M_{24} \\ M_{31} & M_{32} & L_3 & M_{34} \\ M_{41} & M_{42} & M_{43} & L_4 \end{pmatrix} \tag{2}$$

With $M_{ij} = M_{ji}$. Ohm's law can then be written :

$$V_i = R_i.I_i + L_i\frac{dI_i}{dt} + \sum_{j=1,j\neq i}^{4} M_{ij}\frac{dI_j}{dt} \tag{3}$$

This simplistic representation, which perfectly characterizes the electromagnetic behavior of the component, is easy to determine using finite element modeling of the component or in a practical setting using an impedance analyzer. In the following, the finite element analysis of the magnetic component is carried out using COMSOL Multiphysics® software and a comparison with the real component is realized.

III. Digital Modeling of ICT

As previously mentioned, the geometrical complexity added to the difficulty of taking into account the high frequency effects (skin effect, proximity effect...) prevents an analytical resolution of the problem to determine the impedance matrices of the ICT [9], [11]. The use of a 3D modeling by the finite element method is then used to characterize the magnetic component.

For modeling, the 3D component was drawn using the software's CAD tool. The Core "E" corresponds to an E43/10/28 from Ferroxcube® ($43\,\mathrm{mm}\times10\,\mathrm{mm}\times28\,\mathrm{mm}$). When modeling, the surrounding air must be considered to evaluate the leakage inductances. In order to avoid having a too large model, an infinite element domain is applied as a boundary condition. A $50\,\mu\mathrm{m}$ air gap is added at the junction of the ferrites. The Fig. 6 represents the modeled 3D geometry.

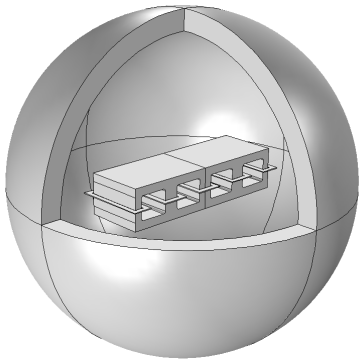


Fig. 6: ICT 3D Model

Each coil is composed of four turns of $2.5\,\mathrm{mm}^2$ diameter and $100\,\mu\mathrm{m}$ thickness, which is a section of $0.25\,\mathrm{mm}^2$. In order to simplify the geometry and to reduce the computation time, the software allows to consider the coils by a homogenized multi-turn coil model by informing the number of coils, the electrical conductivity as well as the section of a coil.

The magnetic problem is solved using Maxwell's equations. The magnetic behavior of materials in view of the low values of induction encountered can be considered as linear and each material is represented by a relative permeability coefficient μ_r. Each material is also represented by an electrical conductivity σ and a relative permittivity ε_r. The Table. I summarizes the physical quantities of the materials used.

TABLE I: Materials properties

	Air	***Core 3C90***	***Copper***
μ_r	1	2000	1
σ	0.00001S/m	0.0001S/m	5.998×10^7S/m
ε_r	1	1	1

The power supply part of each coil is realized with the SPICE tool of COMSOL Multiphysics® software. The four supply voltages of each coil are of the same amplitude ($75\,\mathrm{V}$) but shifted to $2\pi/4$ between them.

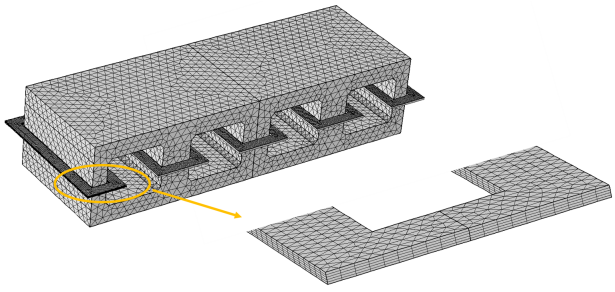


Fig. 7: 3D Model meshing

Meshing is an important aspect of finite element modeling. It must take into account the gradients related to the physics in order to correctly characterize the system. Considering the dimensions of the magnetic core, its mesh can be simply realized with tetrahedral elements. On the other hand, the mesh of the conductors is more complex and requires special attention. Indeed, the Skin effect, the Proximity effect... requires a fine mesh to account for these phenomena. Considering the ratio Length/Thickness or Width/Thickness which is very large, a mesh by extrusion by imposing the number of elements on the thickness seems more appropriate. The Fig. 7 shows the mesh of the ICT.

To determine the impedance matrices of the system, frequency simulations are performed. The excitation frequency is the only variable parameter for this type of simulation. The rest of the paper describes the results of this modeling.

IV. Simulation results

This simulation allows to model the electromagnetic behavior of the inter cell transformer in order to evaluate the induction levels, the inductance matrices according to the electrical excitation parameters (frequency, amplitude) allowing to define the possible use ranges. The simulations are performed with an accuracy of 0.1%.

A. Induction in Inter Cell Transformer

The Fig. 8 shows the induction in the magnetic core for a sinusoidal supply voltage of $75\,\mathrm{V}$ with a frequency of $250\,\mathrm{kHz}$.

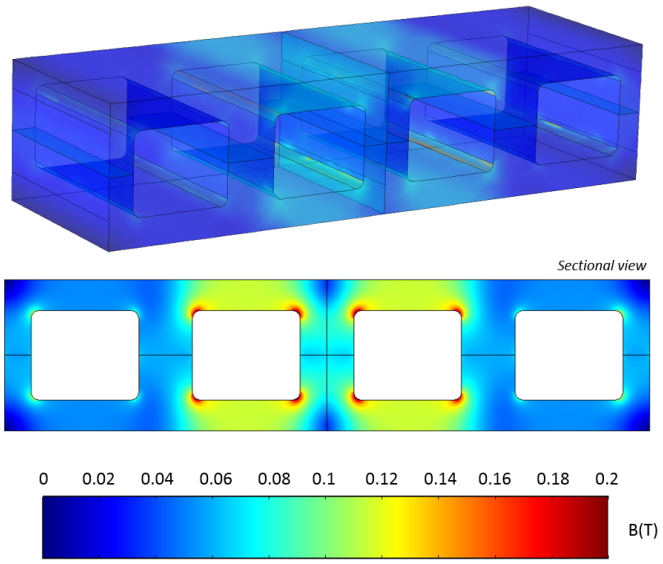


Fig. 8: ICT induction B

The central parts of the core show a higher induction varying around $0.12\,\mathrm{T}$. Logically, the flux in the central parts is more important due to the geometry of the core and the centralisation of the fluxes in this area. In simulation there are edge effects with a much higher induction of up to $0.2\,\mathrm{T}$. In reality, this local saturation is not possible. Indeed, the linear model used for the simulation does not lead to magnetic saturation of the core in these areas. In practice, this saturation exists and the field lines would be distributed differently due to the local permeability decrease of the material slightly increasing the induction in the different legs.

However, the maximum induction of $0.12\,\mathrm{T}$, far from saturation of the magnetic core, shows the possibility of using this system in a buck-boost converter to transfer power between the photovoltaic panels and the battery.

B. Inductances in Inter Cell Transformer

To determine the inductance matrix numerically using finite element modelling, it is sufficient to supply each coil one by one. Thus, the self-inductance is the imaginary part ($\mathfrak{Im}$) of the voltage to current ratio of the coil in question. The mutual inductances are equal to the ratio of the voltage of the no-powered coil to the current in the powered coil.

$$L_i = \frac{1}{\omega}\mathfrak{Im}\left(\left|\frac{V_{\mathrm{Coil}_i}}{I_{\mathrm{Coil}_i}}\right|\right) \tag{4}$$

$$M_{ij} = \frac{1}{\omega}\mathfrak{Im}\left(\left|\frac{V_{\mathrm{Coil}_j}}{I_{\mathrm{Coil}_i}}\right|\right) \tag{5}$$

For a supply voltage frequency of $250\,\mathrm{kHz}$ the inductance matrix is :

$$(L) = \begin{pmatrix} 44.49 & -15.64 & -11.95 & -15.64 \\ -15.64 & 37.04 & -15.48 & -4.92 \\ -11.95 & -15.47 & 43.86 & -15.47 \\ -15.64 & -4.92 & -15.48 & 37.04 \end{pmatrix} [\mu\mathrm{H}] \tag{6}$$

The resulting matrix is symmetrical. For each line of the matrix, we have a good distribution of the self-inductance through the mutual inductances ($L_i = \sum M_{ij}$) showing the capacity of the magnetic circuit to channel the flux with a very low leakage flux. The principle of distributed the coil 1 on both sides of the magnetic core makes it possible to better distribute the mutual inductances and to have the mutual inductances equal to each other, which is normally impossible with a non-symmetrical core shape like the one used here. Only the value of the mutual M_{24} is low due to the distance between the two coils. However, the result obtained seems to be a good compromise between ease of realisation and performance.

Simulations for several operating frequencies up to $500\,\mathrm{kHz}$ have shown that this inductance matrix hardly varies. This is due to the fact that the currents induced in the material are very small and do not affect the permeability of the magnetic core [12].

V. Experimental results

The comparison between simulation and experimental results can be difficult. Indeed, many aspects such as geometrical tolerance, length of measure wires and contact connectors are not considered in the simulation and can modify the results. It is therefore necessary to validate this modeling by comparison with measurements on the real object. The model thus dimensioned was carried out within the laboratory in order to validate the design by the finite element modeling.

A. Experimental setup

As indicated at the beginning of the article, the magnetic core is formed from four "E" of reference "Ferroxcube® E43/10/28" whose material is 3C90. The coils are designed on a double layer PCB. They are realized to respect the direction of the fluxes as mentioned in Fig. 4. A custom-made support was designed using Solidworks® software and manufactured by 3D printing with the help of the technological platform of the University of Montpellier PRO3D®. It allows to maintain between them the four cores "E" by means of a tightening of screws. An air gap of $50\,\mu m$ is added to the interface of the "E" using a Kapton film. The Fig. 4 represents an exploded view of the whole made with Solidworks®.

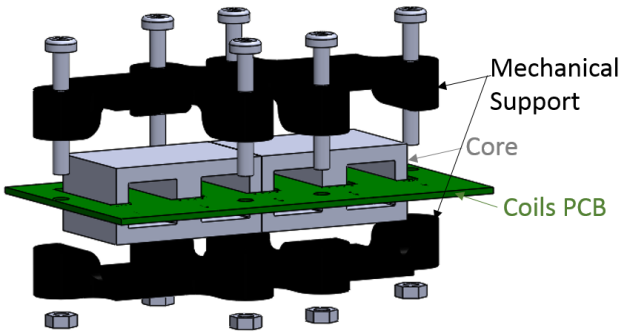


Fig. 9: Exploded view of Inter Cell Transformer

The final assembly was done in the laboratory. See Fig. 10.

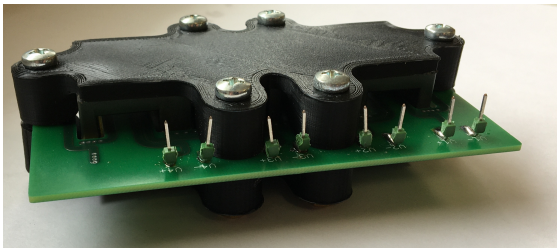


Fig. 10: Experimental Inter Cell Transformer

In order to measure the inductance matrix an impedance analyzer HM8118 from ROHDE & SCHWARTZ® was used. The measurement schematics are given in Fig. 11. Although the inductance matrix is symmetrical, the sixteen measurements of self and mutual inductances have been measured to detect a possible unbalance.

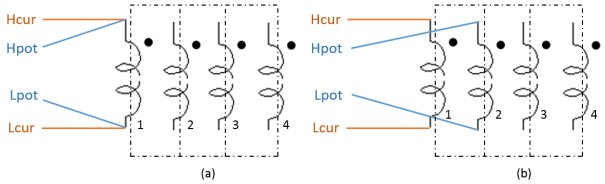


Fig. 11: Measurement schematics : (a) - self inductance measurement, (b) - mutual inductance measurement

Hcur/Lcur are the current injection ports of the HM8118 and Lpot/Hpot are the measurement ports. The Fig. 11 shows an example of measuring the self-inductance L_1 and the mutual inductance M_{12}. Simply move Hpot and Lpot on the other coils to measure M_{13} and M_{14}.

B. Inductance matrix measurement

The set of measurements to determine the inductance matrix was carried out and the results are presented in Eq. 7.

$$(L) = \begin{pmatrix} 44.29 & -15.09 & -11.22 & -15.33 \\ -14.97 & 37.01 & -15.12 & -4.61 \\ -11.22 & -15.11 & 43.68 & -15.30 \\ -15.32 & -4.60 & -15.35 & 37.41 \end{pmatrix} [\mu H] \quad (7)$$

From these measurements it appears that, as expected, the matrix is symmetrical, taking into account the geometry and the measurement errors. The results are consistent with those determined in simulation. There are some errors of up to 6.8% in some cases, but the overall error is only 2.87% which is quite acceptable. The differences between the experimental measurements and the values determined in simulation can be explained by geometrical tolerances between the real product and the modelled geometry, the magnetic behaviour B(H) which can be different in practice, measurement errors attributable to the measuring device, etc. However, these differences have no impact on the overall calculation of the Inter Cell Transformer and in particular on the calculation of the magnetising and leakage inductances of the component.

As in the simulation, the self-inductances are close to the sum of the mutual inductances showing the capacity of the magnetic core to channel the flux. A disparity will occur in the distribution of the mutual inductances which will result in the frequency component equal to four times the switching frequency not being cancelled. However, the result remains consistent and shows the feasibility of this solution for use in a power converter. The ease of practical implementation is the main advantage of this solution.

VI. Conclusion

This article is the first step in the development of a power converter for a marine drone. This type of application requires a lot of energy in a small volume. The solution proposed

here by the use of a multi-cell converter seems to be an interesting approach thanks to the use of an inter cell transformer. The main advantage of the component described here is its simplicity of construction, which is often an obstacle to the construction of this type of component. An ICT design approach using a finite element modelling method has been shown here. It allows a considerable gain in the design of magnetic components. This modelling made it possible to validate the concept of this Inter Cell Transformer. The dimensioned component was made and measurements of the magnetic behaviour were made. The modelling/experimentation confrontation shows convincing results with minimal errors further validating the concept of this magnetic component. Through this article, we have been able to show the effectiveness of finite element modelling design in the realisation of specific magnetic components.

ACKNOWLEDGMENT

This research was supported by Occitanie région by a FEDER program N°: ESR_R&S_DF-000035-2017-006565.

Thanks to the PRO3D platform of the University of Montpellier for the realization of the parts in 3D printing.

REFERENCES

[1] G. Zhu, B. McDonald and K. Wang, "Modeling and Analysis of Coupled Inductors in Power Converters," 2009 Twenty-Fourth Annual IEEE Applied Power Electronics Conference and Exposition, 2009, pp. 83-89, doi: 10.1109/APEC.2009.4802637.

[2] Jieli Li, C. R. Sullivan and A. Schultz, "Coupled-inductor design optimization for fast-response low-voltage DC-DC converters," APEC. Seventeenth Annual IEEE Applied Power Electronics Conference and Exposition (Cat. No.02CH37335), 2002, pp. 817-823 vol.2, doi: 10.1109/APEC.2002.989338.

[3] T. Martire, J. Laurentie, M. Jebli, L. Boyer and M. Petit, "Design of a 4-phase intercell transformer converter for a space charge measuring system," 2018 IEEE International Conference on Industrial Technology (ICIT), 2018, pp. 676-681, doi: 10.1109/ICIT.2018.8352259.

[4] B. Cougo, V. Costan, T. Meynard, F. Forest and E. Laboure, "A new intercell transformer for interleaved converters," 2009 13th European Conference on Power Electronics and Applications, 2009, pp. 1-10.

[5] Y. Shi, H. Li, L. Wang and Y. Zhang, "Intercell Transformer (ICT) Design Optimization and Interphase Crosstalk Mitigation of a 100-kW SiC Filter-Less Grid-Connected PV String Inverter," in IEEE Open Journal of Power Electronics, vol. 1, pp. 51-63, 2020, doi: 10.1109/OJPEL.2020.2973074.

[6] K. -B. Park, F. D. Kieferndorf, U. Drofenik, S. Pettersson and F. Canales, "Optimization of LCL Filter With Integrated Intercell Transformer for Two-Interleaved High-Power Grid-Tied Converters," in IEEE Transactions on Power Electronics, vol. 35, no. 3, pp. 2317-2333, March 2020, doi: 10.1109/TPEL.2019.2926312.

[7] Pit-Leong Wong, Peng Xu, P. Yang and F. C. Lee, "Performance improvements of interleaving VRMs with coupling inductors," in IEEE Transactions on Power Electronics, vol. 16, no. 4, pp. 499-507, July 2001, doi: 10.1109/63.931059.

[8] In Gyu Park and Seon Ik Kim, "Modeling and analysis of multi-interphase transformers for connecting power converters in parallel," PESC97. Record 28th Annual IEEE Power Electronics Specialists Conference. Formerly Power Conditioning Specialists Conference 1970-71. Power Processing and Electronic Specialists Conference 1972, 1997, pp. 1164-1170 vol.2, doi: 10.1109/PESC.1997.616895.

[9] T. Meynard, B. Cougo, F. Forest and E. Labouré, "Parallel multicell converters for high current: Design of intercell transformers," 2010 IEEE International Conference on Industrial Technology, 2010, pp. 1359-1364, doi: 10.1109/ICIT.2010.5472516.

[10] E. Laboure, A. Cuniere, T. A. Meynard, F. Forest and E. Sarraute, "A Theoretical Approach to InterCell Transformers, Application to Interleaved Converters," in IEEE Transactions on Power Electronics, vol. 23, no. 1, pp. 464-474, Jan. 2008, doi: 10.1109/TPEL.2007.911786.

[11] B. Cougo, "Design and optimization of intercell transformers for parallel multicell converters", PhD Thesis, University of Toulouse, INP, LAPLACE Laboratory, Toulouse, France, 2010.

[12] L. Havez, E. Sarraute and D. Flumian, "3D Virtual Identification of a Power Inter Cell Transformer", Proceedings of PCIM Europe 2015, International Exhibition and Conference for Power Electronics, Intelligent Motion, Renewable Energy and Energy Management, May 19-20, 2015, Nuremberg (GERMANY), pp. 578-585.